

A MODEL FOR THE SHAPE OF THE FOURIER AMPLITUDE SPECTRUM OF ACCELERATION AT HIGH FREQUENCIES

BY JOHN G. ANDERSON AND SUSAN E. HOUGH

ABSTRACT

At high frequencies f the spectrum of S-wave accelerations is characterized by a trend of exponential decay, $e^{-\kappa f}$. In our study, the spectral decay parameter κ shows little variation at a single station for multiple earthquakes at the same distances, but it increases gradually as the epicentral distance increases. For multiple recordings of the San Fernando earthquake, κ increases slowly with distance, and κ is systematically smaller for sites on rock than for sites on alluvium. Under the assumption that the Fourier spectrum of acceleration at the source is constant above the corner frequency (an ω^{-2} source model), the exponential decay is consistent with an attenuation model in which Q increases rapidly with depth in the shallow crustal layers.

INTRODUCTION

The shape and amplitude of the Fourier amplitude spectrum of strong ground acceleration is recognized as useful for various applications to earthquake engineering (McGuire, 1978). This acceleration spectrum also contains fundamental information about physical processes at the earthquake source and wave propagation in the crust of the earth. Yet at high frequencies, we still do not have a satisfactory model for the shape of the acceleration spectrum. By the shape of a spectrum we refer to a smooth trend through the spectrum; the fine structure which is superimposed on this trend is not meant to be included.

At low frequencies and sufficiently far from the fault, the inevitable result of an elastic rebound source model is that the acceleration spectrum increases as ω^2 , where $\omega = 2\pi f$ and f is the frequency of ground motion. For example, a widely employed model by Brune (1970) relates the coefficient of this ω^2 trend to the seismic moment, M_0 , and relates the corner frequency (f_0) where this ω^2 trend terminates to a stress drop parameter at the source. Above the corner frequency, Trifunac (1976) and McGuire (1978) have carried out empirical regressions for the shape of the acceleration spectrum but these regressions do not yield much insight into the physical processes which are involved. Hanks (1979, 1982) suggests that, in general, the acceleration spectrum is flat above the corner frequency to a second corner frequency (f_{max}) above which the spectrum decays rapidly.

In the next section, we propose a parametric shape for the acceleration spectrum at high frequency. Our model is characterized by one parameter, which we designate as the spectral decay parameter κ . Recognition and study of this parameter were motivated in part by the observations that most spectra observed in the 1981 Santa Barbara Island earthquake appear to fall off exponentially (Anderson, 1984). Subsequent sections explore the systematic behavior of κ for the S-wave portion of the accelerogram. We also recognize a plausible attenuation model to explain the observations but intentionally avoid introducing the terminology and notation of that model into the observation sections of this paper.

SPECTRAL SHAPE AT HIGH FREQUENCIES

Figure 1 shows the Fourier amplitude spectrum of acceleration for the S16°E component of the Pacoima Dam accelerogram from the 1971 San Fernando, Cali-

foria, earthquake. Figure 1A shows the spectrum plotted on log-log axes. Based on a figure of this type, Hanks (1982, Figure 2) selects f_{max} for this record to be near 10 Hz. In Figure 1B, the frequency axis is linear. On these axes, the dominant trend is a linear decrease of the log of spectral amplitude with frequency, and there is no apparent additional slope break in the vicinity of 10 Hz. In some cases, the dominant trend of exponential decay is initiated near f_0 , but on other spectra it begins at some higher frequency. It is, therefore, useful to label the frequency above which the spectral shape is indistinguishable from exponential decay. Here we call this frequency f_E . We do not ascribe any fundamental importance to f_E , and pay little attention to it in the rest of this paper. Considering the amplitude of the fine

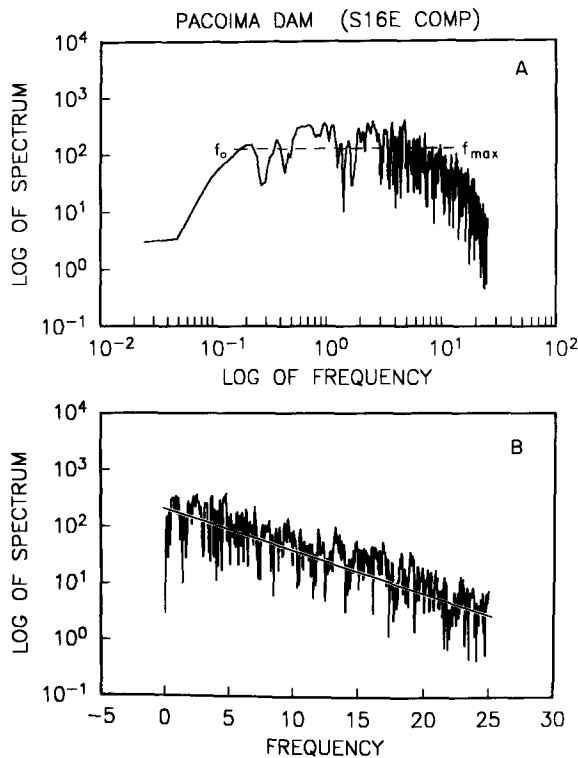


FIG. 1. Fourier amplitude spectrum of acceleration for the S16°E component of the Pacoima Dam accelerogram, San Fernando, California, earthquake of 9 February 1971. Accelerogram was digitized by hand. (A) Log-log axes. (B) Linear-log axes.

structure to the spectrum (Figure 1), it is difficult to determine meaningful trends over narrow frequency bands (e.g., bandwidth less than about 3 to 5 Hz). Thus the identification of f_E , like that of f_{max} , is to some extent subjective. On Figure 1, f_E may occur between 2 and 5 Hz. Thus, on this spectrum, f_E is distinctly less than the value for f_{max} which was identified by Hanks (1982).

Figure 2 is the equivalent of Figure 1, but for the spectrum of an accelerogram recorded at Cucapah, Baja California, Mexico, from the June 1980 earthquake ($M_L = 6.1$) in the Mexicali Valley, across the international border from the Imperial Valley, California. These data are described by Anderson *et al.* (1982). The accelerograph in this case is a digital recorder (Kinometrics DSA-1) which samples the output of a force-balance accelerometer (natural frequency 50 Hz) at a rate of 200 samples/sec, so that the Nyquist frequency is 100 Hz. The least count is about 0.5

cm/sec². Because the response of the force-balance sensor is flat to 50 Hz, no instrument correction has been applied to this record. Because of the highly accurate digital recording, there is little uncertainty about the reliability of the digitization on this record, as there might be for hand-digitized data (e.g., Berrill and Hanks, 1974; Sacks, 1980; Cormier, 1982).

Figure 2A shows the same general properties as Figure 1A, although the window in this case was not long enough to establish a low-frequency asymptote at frequencies less than the corner frequency f_0 . By analogy to Figure 1A, one would pick f_{max} at about 10 Hz for the spectrum in Figure 2A. Figure 2B again shows a predominantly exponential decrease in spectral amplitude, in this case from 1 to 40 Hz. Below

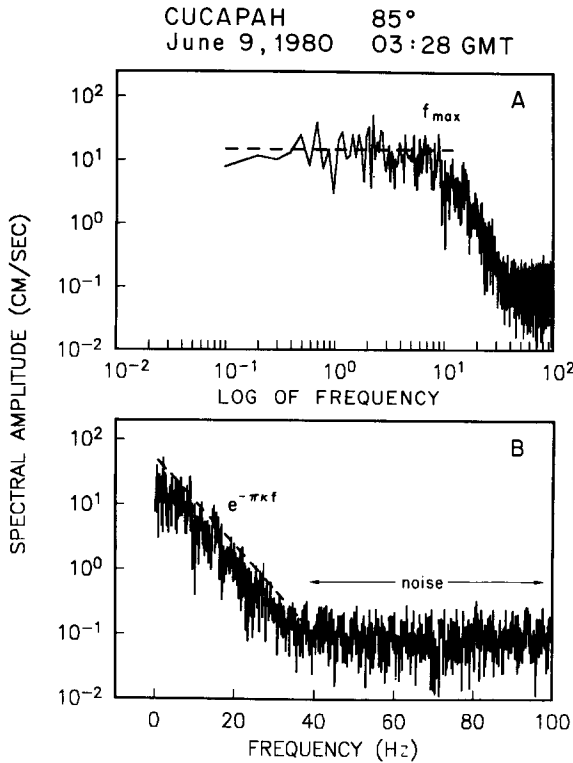


FIG. 2. Fourier amplitude spectrum of the N85°E component of strong ground acceleration recorded at Cucapah during the Mexicali Valley earthquake of 9 June 1980 ($M_L = 6.2$). Accelerograph was a digital recorder which samples at a rate of 200/sec. (A) Log-log axes. (B) Linear-log axes.

about 6 Hz, there is again room to define, at a lower confidence level, a trend which diverges from the exponential trend which dominates over the full frequency band. At 40 Hz the exponential trend intersects spectral amplitudes of about 0.1 cm/sec, corresponding to the least count digitization level, and above 40 Hz the spectrum is flat, as is appropriate for a digitization process with random round-off errors at an amplitude of ± 0.5 least count.

Based on Figures 1 and 2, and many comparable spectral plots, we hypothesize that to first order the shape of the acceleration spectrum at high frequencies can generally be described by the equation

$$a(f) = A_0 e^{-\pi \kappa f} \quad f > f_E \tag{1}$$

where A_0 depends on source properties, epicentral distance, and perhaps other factors. The systematic behavior of the spectral decay parameter κ is explored in the next three sections of this paper.

METHOD

We studied shear-wave spectra for the horizontal components of strong ground acceleration from 98 sites around the 1971 San Fernando earthquake, ten events recorded at Ferndale, ten events recorded at El Centro, and five events recorded at Hollister. All records are corrected accelerograms from the Volume II data tape prepared by the Earthquake Engineering Research Laboratory of California Institute of Technology (EERL, 1971).

Fourier transforms of the shear waves were computed from accelerograms. The time window was chosen to include only direct S -wave arrivals. In cases where the transition from direct S -wave arrivals to coda was not readily apparent, our choice for the time window favored including coda rather than possibly eliminating direct arrivals. Spectral shape was found to be fairly insensitive to the time window length as long as it was reasonably chosen. The value of κ at stations ~ 40 km from the epicenter of the San Fernando earthquake showed no correlations with time window length. The transforms were computed with a standard Fast Fourier transform routine after a cosine taper was applied to the raw data and the time series were padded out to powers of two with zeroes. The spectra were plotted from 0 to 25 Hz (Nyquist frequency = 25 Hz).

To obtain the spectral decay parameter, linear least-squares fits to the spectra were obtained. A 2- to 12-Hz interval was used for the El Centro, Ferndale, and Hollister records. The corner frequencies for all of the earthquakes we considered are less than 2 Hz. Frequencies higher than 12 Hz were considered potentially unreliable on some of these records in these data sets for reasons to be discussed later. For the San Fernando records, the interval used for regression was 2 to 18 Hz.

Values of the slopes were converted to the spectral decay parameter, κ , and subsequently plotted against epicentral distance to evaluate distance-dependence. To quantify trends, we found a linear regression between κ and distance, R , even though we do not believe a linear relationship is the definitive dependence of κ on R . For the multiple event data, these straight lines were fit directly. The San Fernando data were averaged within 10-km distance bands and then fit with straight lines. This latter procedure reduces the weight of the distance ranges which are represented by large numbers of stations. Regression done on the complete data sets yielded similar results.

RESULTS: SINGLE STATION AND MULTIPLE EVENTS

Figures 3 through 9 illustrate results for records of earthquakes at multiple distances from a single station. Figure 3 is a map of the vicinity of the El Centro accelerograph, showing locations of the station, epicenters of ten earthquakes which were recorded on the accelerograph, and generalized surficial geology. Corresponding S -wave spectra and least-squares fits are shown in Figure 4. Figure 5 is a map of the Ferndale vicinity, and Figure 6 shows corresponding spectra for ten earthquakes which have been recorded there. Locations of the earlier earthquakes recorded at El Centro and Ferndale may have substantial errors. The 1934 and 1954 earthquakes at El Centro are shown at the relocated epicenters of Leeds (1979). These epicenters may be more reliable than others among the earlier earthquakes on these maps.

Figure 7 is a map of the Hollister vicinity and Figure 8 shows corresponding spectra for five earthquakes recorded at Hollister. Finally, Table 1 and Figure 9 show measured values of κ as a function of distance for all three stations.

Figure 4 shows spectra for both components of the El Centro station. On these spectra, a linear trend dominates the spectral shapes for frequencies between 2 and

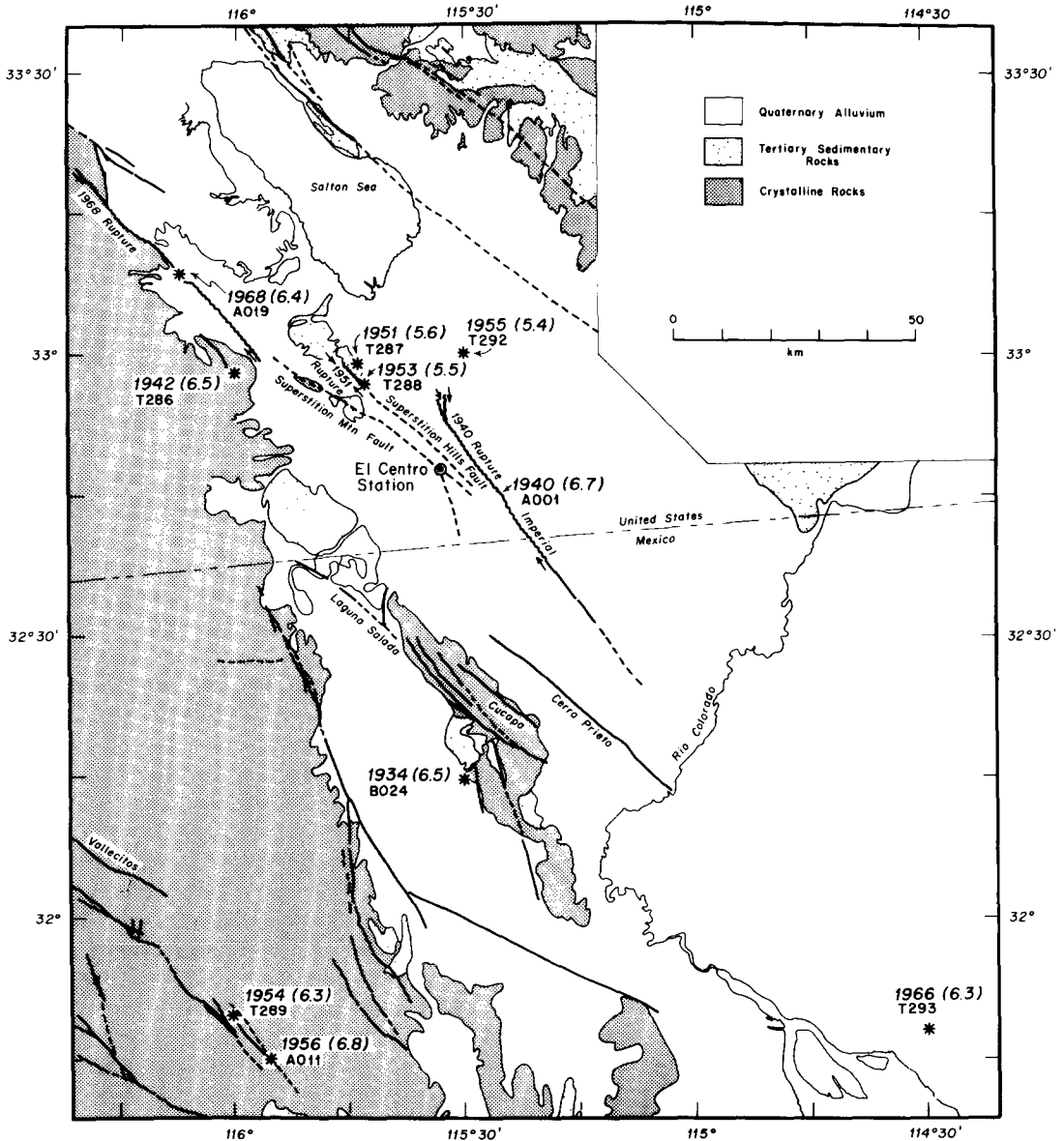


FIG. 3. Map of Imperial Valley, California-Mexico showing generalized geological features. Epicenters (asterisk) from Leeds (1979) or Hileman *et al.* (1973) are shown with year and magnitudes of earthquakes which have generated accelerograms at the El Centro station. Accelerogram number on the Caltech tapes is given below year. The 1940 and 1968 ruptures are from Jennings (1975).

12 Hz. Spectra for the 1934, 1940, and 1942 earthquakes (records B024, A001, and T286, respectively) have a nearly level trend starting at frequencies between 12 and 15 Hz. Likewise in Figure 6 many of the spectra, and most conspicuously the spectra for the earliest earthquakes, appear to assume a nearly level trend starting at

frequencies as low as about 12 Hz. In Figure 8 all of the spectra deviate above the linear trend starting at between 12 and 15 Hz. In Figure 2, similar behavior resulted from the digitization, thus suggesting that digitization has also caused level spectral trends on these accelerograms.

An estimate for the typical range for the Fourier amplitude of digitization noise for these hand-digitized accelerograms has been presented by Berrill and Hanks (1974). Noise amplitudes under the digitization conditions of these accelerograms

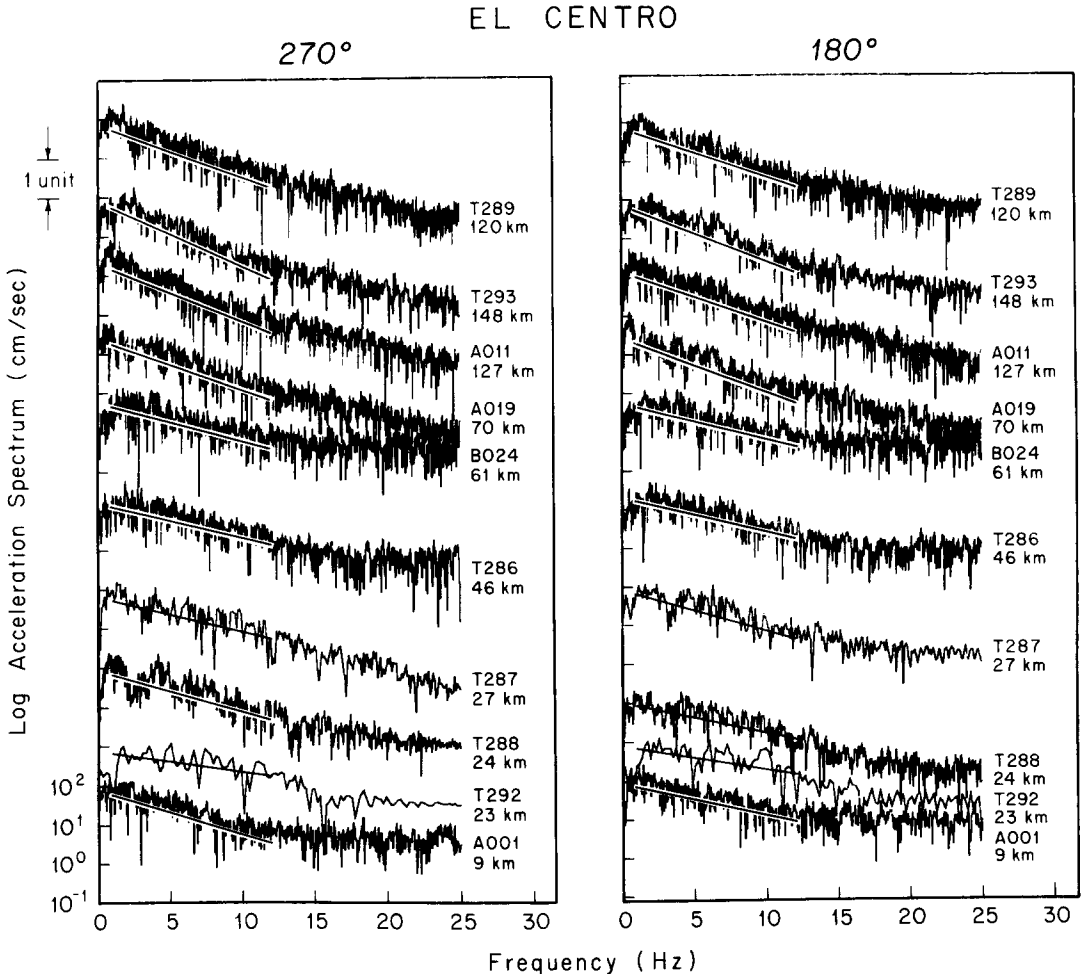


FIG. 4. Fourier amplitude spectra of *S*-wave accelerograms corresponding to epicenters from Figure 3. Record number and distance from the accelerograph are indicated to *right* of each spectrum. Each spectrum is offset by two logarithmic units from the spectrum immediately below. Superimposed on each spectrum is a linear, least-squares fit over the frequency band 2 to 12 Hz.

and the signal window employed in our study decrease smoothly from about 0.3 ± 0.07 cm/sec at 1 Hz to 0.18 ± 0.06 cm/sec at 12 Hz, and 0.11 ± 0.03 cm/sec at 24 Hz. Deviations of *S*-wave spectra above an exponential decay approximately coincide with these levels for all Hollister spectra (Figure 8) and for El Centro and Ferndale spectra of earthquakes recorded after 1949 (Figures 4 and 6).

All of the pre-1948 spectra from El Centro and Ferndale form a trend parallel to the digitization noise but the amplitude of this trend exceeds the amplitudes found

by Berrill and Hanks (1974). It turns out that instrumental characteristics of the accelerographs at El Centro and Ferndale were modified once. Before the modification, the undamped natural frequency of each sensor was about 10 Hz (e.g., Bodel, 1944). Beginning in 1942, the U.S. Coast and Geodetic Survey began to modify its accelerographs to reduce the gain at selected stations. This modification was made at El Centro and at Ferndale in late 1948 or early 1949, based on a review of instrument constants published in the series *United States Earthquakes* (see Mur-

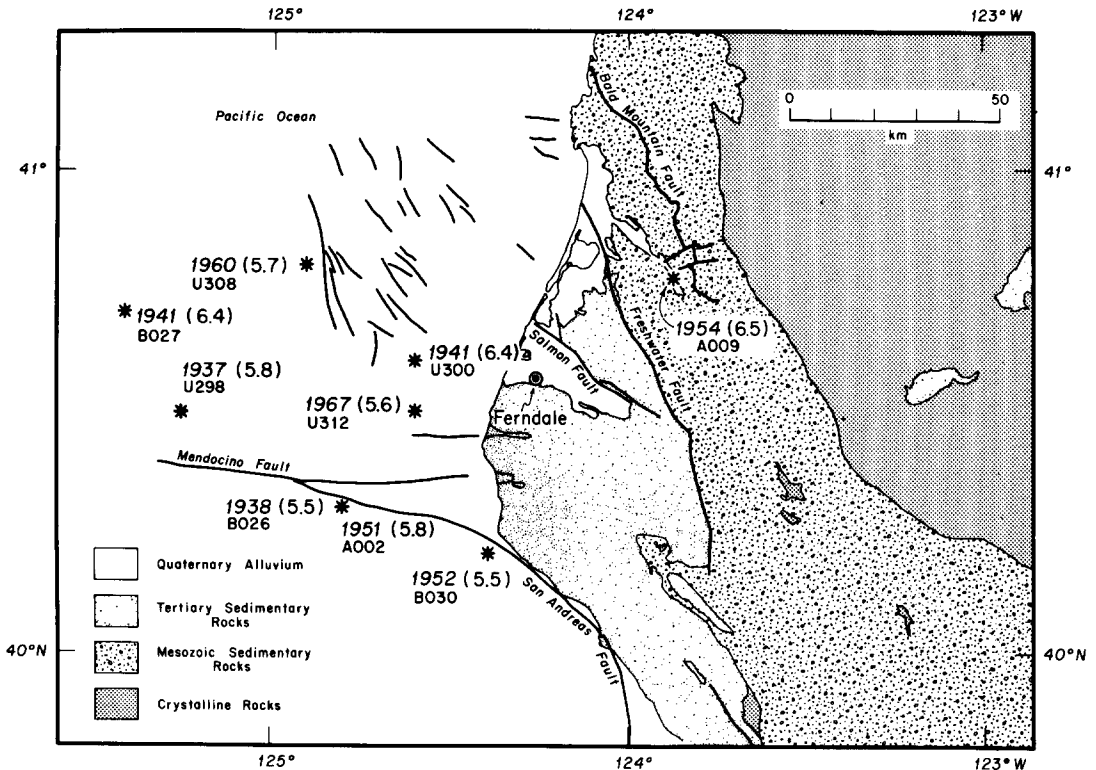


FIG. 5. Map of Cape Mendocino, California, showing generalized geological features. Epicenters from Trifunac and Lee (1978) are identified with the same notations as in Figure 3 and represent earthquakes which have produced accelerograms on the Ferndale accelerograph. The 1934, $M = 6.0$ earthquake (Record U294) was located off map at 41.7°N , 124.6°W . Real *et al.* (1978) location for the 1938 earthquake is 40°N , 124°W , about 75 km from the epicenter shown here.

phy and Ulrich, 1951a, b). Subsequently, the natural frequencies of the sensors were between 15 and 16 Hz. Thus, if we assume that the digitization and instrument correction procedure for the pre-1948 earthquakes leads to digitization noise above the level described by Berrill and Hanks (1974), the deviations of spectra in Figures 4, 6, and 8 above the model of exponential decay are all explained by digitization noise.

For the 1953 event, the north-south component at El Centro may have been working improperly based on the appearance of the original accelerogram in Murphy and Cloud (1955) and spectral levels nearly an order of magnitude less than for the east-west component. The same trace was defective for the record of the 21 July 1952 Kern County earthquake (Murphy and Cloud, 1954). We have thus not included that measurement of κ on Figure 9, even though it is consistent with other values.

The El Centro station data in Figure 4 show that the spectral slopes of the two

horizontal components of S waves from an earthquake are similar. Spectra in Figure 4, generally arranged from farthest to nearest, show a weak but clear distance dependence of the spectral shape, which is confirmed in Table 1 by the numerical values of the spectral decay parameters. The least-squares line through these data on Figure 9 has the equation $\kappa = 0.054 \text{ sec} + (0.00041 \text{ sec/km})R$, where R is the source-to-station distance.

Accelerograms which have been recorded at Ferndale are primarily from offshore locations (Figure 5), and many of the epicenters are not well controlled. Spectra (Figure 6) show a less conspicuous increase of κ with distance than for El Centro

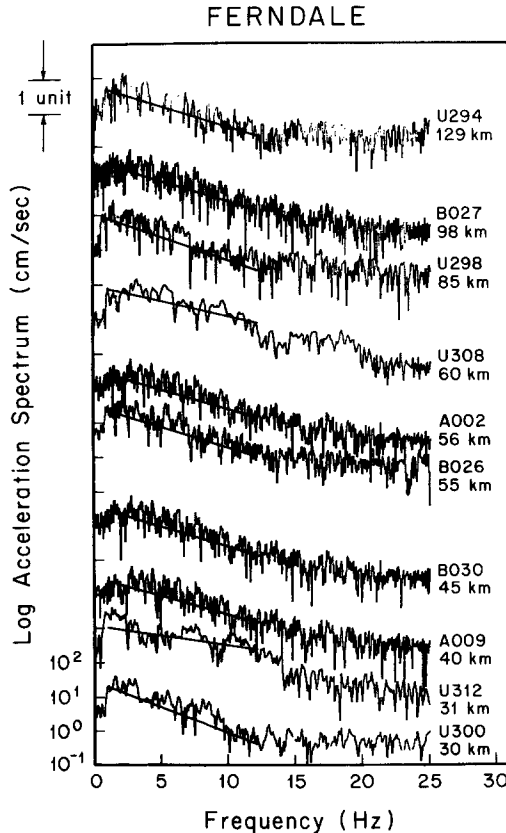


FIG. 6. S -wave acceleration spectra from Ferndale site for earthquakes on Figure 5. Please refer to Figure 4 caption for other notation.

records. The least-squares fit to the Ferndale data on Figure 9 is $\kappa = 0.075 \text{ sec} + (0.00016 \text{ sec/km})R$. Spectra from Hollister (Figure 8) do not show a conclusive change in the spectral decay parameter with distance, but all the accelerograms were obtained at distances of less than 40 km.

Figure 9 summarizes the three studies of multiple recordings at a single station. At El Centro, Ferndale, and Hollister, the spectral decay parameter exhibits a common type of behavior. Within the resolution of the data, κ tends toward a finite value as epicentral distance approaches zero; we interpret this finite value as a characteristic of the subsurface geological structures. The term "subsurface geological structure" is used in the sense employed by Dobrin (1960) to refer to geological conditions below and near the site within distances on the order of hundreds of

meters to a few kilometers. In addition to the subsurface geology effect, a path-distance effect also seems to be present and causes κ to increase gradually with distance. The existence of this systematic behavior suggests that the source spectral shapes of the several earthquakes probably had identical trends between the frequencies of 2 and 12 Hz.

TABLE 1
SPECTRAL DECAY PARAMETERS FOR ACCELEROGRAMS RECORDED
AT HOLLISTER, FERNDAL, AND EL CENTRO

Date	Record	Distance	Magnitude	κ_1	κ_2
HOLLISTER					
03/09/49	U301	19.9	5.3	0.0850	
04/25/54	U305	29.1	5.3	0.0828	
01/19/60	U307	8.5	5.0	0.0865	
04/08/61	U309	19.8	5.6	0.0667	
12/18/67	U313	39.0	5.8	0.0880	
FERNDAL					
10/07/51	A002	56.3	5.8	0.0858	
12/21/54	A009	40.4	6.5	0.0821	
09/11/38	B026	55.3	5.5	0.0909	
02/09/41	B027	98.4	6.4	0.0909	
09/22/52	B030	45.2	5.5	0.0887	
07/06/34	U294	128.9	6.0	0.0923	
02/06/37	U298	85.1	5.8	0.1019	
10/03/41	U300	29.8	6.4	0.1114	
06/05/60	U308	60.3	5.7	0.0667	
12/10/67	U312	30.6	5.6	0.0447	
EL CENTRO					
05/19/40	A001	9.3	6.7	0.0608	0.0806
02/09/56	A011	126.9	6.8	0.0945	0.1077
04/08/68	A019	69.8	6.4	0.1011	0.0938
12/30/34	B024	60.8	6.5	0.0682	0.0711
10/21/42	T286	46.5	6.5	0.0645	0.0645
01/23/51	T287	27.5	5.6	0.0770	0.0630
06/13/53	T288	23.6	5.5	0.0591	0.0751
11/12/54	T289	119.8	6.3	0.0923	0.0975
12/16/55	T292	23.5	5.4	0.0452	0.0369
08/07/66	T293	148.1	6.3	0.1048	0.1217

RESULTS: SAN FERNANDO EARTHQUAKE

The San Fernando earthquake represents a situation in which multiple recordings have been made of a single event. Azimuthal variations in κ resulting from the source function were assumed negligible even though radiation at frequencies of 4 Hz and lower might be affected by source directivity (Berrill, 1975). This earthquake was used to study the effect of variable local geology and distance on κ . A map showing station locations and generalized geology has been prepared by Hanks (1975).

About 90 per cent of the spectra from the San Fernando records have an average trend which is modeled well by equation (1). The other 10 per cent of the records often appear to follow the same trend, except for a superimposed bulge which we

tentatively identify as a site amplification effect. Figure 10 shows one of the more conspicuous examples of Fourier spectra with a relatively large apparent amplification of this type. Smaller broadband resonances may be unrecognized, and we conjecture that such resonances may add noise to determinations of κ .

Table 2 and Figure 11 summarize values of κ obtained from the San Fernando earthquake. Table 2 also lists the distance, the window length employed (T), and site classification, S . In Figure 11, the stations were grouped into three categories: alluvium ($S = 0$), consolidated sedimentary rock ($S = 1$), and hard (igneous or metamorphic) rock ($S = 2$), following the site classification of Trifunac and Brady (1975). Stations listed as being on sedimentary rocks actually include sites on

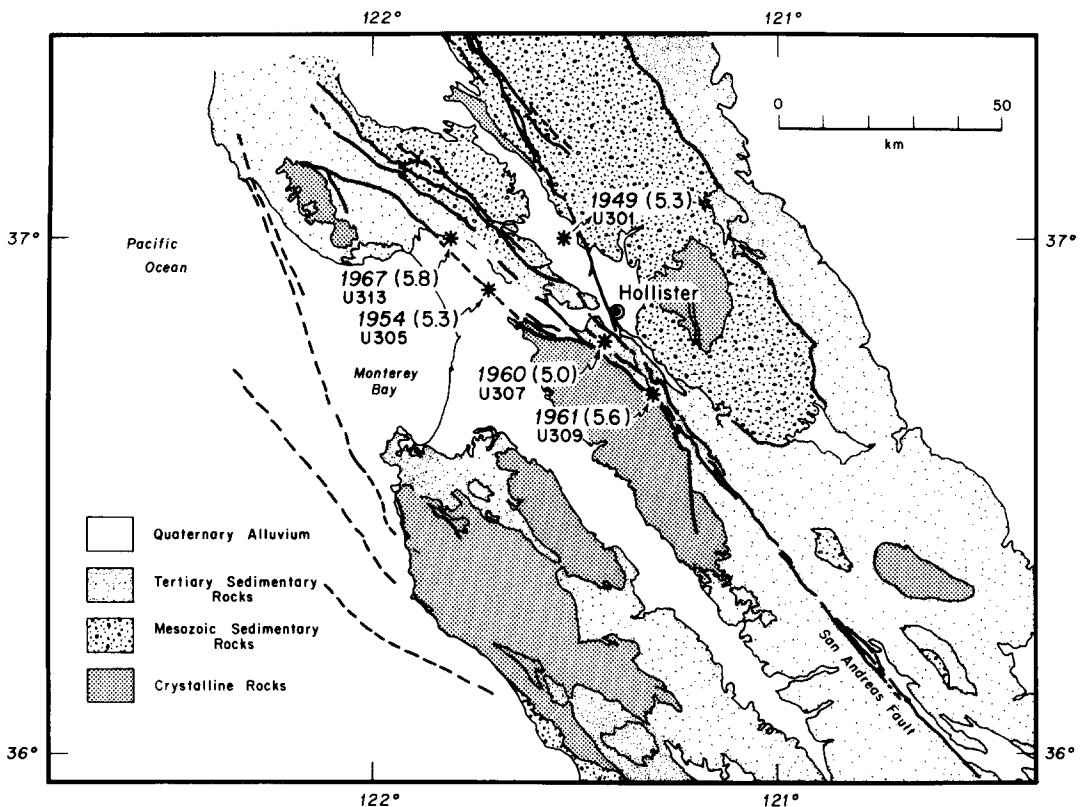


FIG. 7. Map of central California showing generalized geological features. Epicenters from Real *et al.* (1978) are identified with the same notation as in Figure 3 and represent earthquakes which have produced accelerograms on the Hollister accelerograph.

shallow alluvium as well as those on consolidated sediments. In this manner, the site classifications of Trifunac and Brady (1975) attempt to account for subsurface geological structure as well as conditions in the immediate vicinity of the site.

Trends in the raw data on Figure 11 resemble trends on Figure 9, except for a larger amount of scatter: κ tends toward a finite intercept and increases slowly with distance. The larger amount of scatter is predictable if a major contribution to κ results from a subsurface geologic structure effect, since subsurface geology is highly variable. Figure 11 also shows average values of κ over 10-km intervals and least-square linear regression through these averages. Numerical values of the regression lines between κ and R are in the figure caption. There is a factor of three difference between the slopes of these regressions for stations on alluvium and on rock. These

differences result in part from different distance ranges involved in the regressions. Considering this and the scatter in the data, it is doubtful that the slope differences are significant. An observation which may be significant is that, averaged over the distance range to 70 km, stations on alluvium ($S = 0$) and consolidated sedimentary rock ($S = 1$) give indistinguishable values for κ while the values of κ for hard rock sites average about 25 per cent lower.

RESULTS: REGRESSIONS FOR FOURIER AMPLITUDE OF ACCELERATION

Spectral shapes which were obtained by the regressions of Trifunac (1976) and McGuire (1978) also show exponential decay with frequency. Discrete points at frequencies greater than 1 Hz from both regressions are illustrated in Figure 12 for

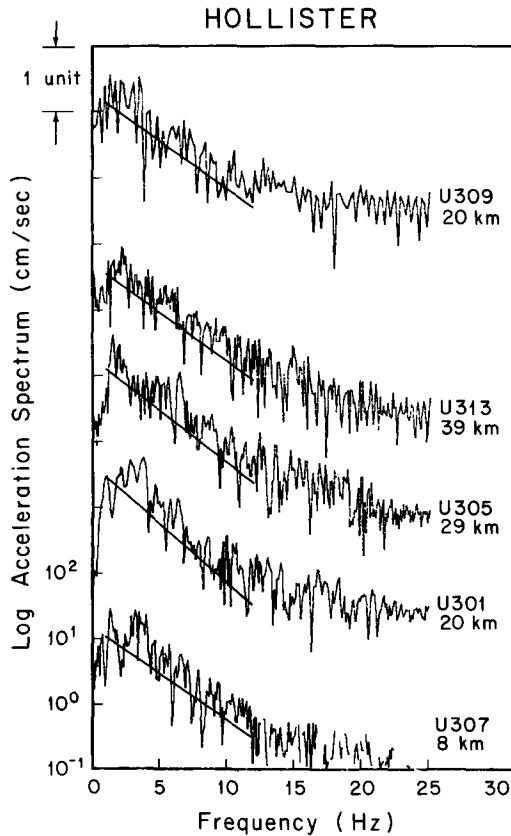


FIG. 8. S-wave acceleration spectra from Hollister site for earthquakes on Figure 7. Please refer to Figure 4 caption for other notation.

a magnitude 6.5 earthquake at 25 and 100 km. For the Trifunac (1976) regression, the mean predicted spectra on soil conditions agree with exponential decay for frequencies from 2 to 15 Hz, and mean predicted spectra on rock conditions agree with exponential decay for frequencies from 5 to 15 Hz. The points at 25 Hz fall above the level consistent with exponential decay, but this may result from noise, as in some of the spectra shown in previous figures. The results from McGuire (1978), shown in Figure 13B, confirm this result. This regression indicates that exponential decay persists to frequencies of 20 Hz at 25 km and for rock sites at 100 km. The results by Trifunac (1976) at 25 km and at 100 km, and results of McGuire (1978) at 100 km anticipate the lower values of the spectral decay

parameter on rock sites, as found in our study. The McGuire results for soil sites anticipate the observed increase of the spectral decay parameter with distance. Numerical values of spectral decay parameters for all lines on Figure 12 are between 0.077 and 0.090 sec, and are slightly higher than values which would have been anticipated based on our results. However, spectra studied by Trifunac and by McGuire were whole record spectra, while we used *S*-wave spectra.

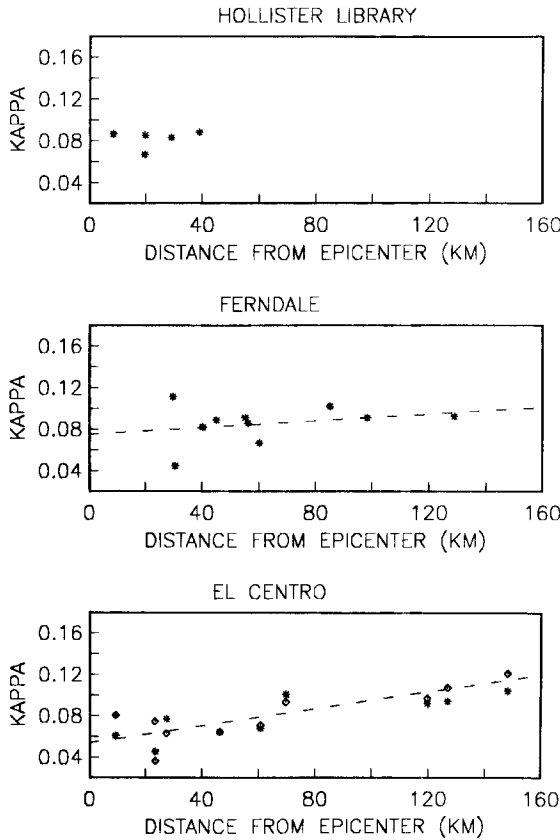


FIG. 9. Values of κ for frequency band 2- to 12-Hz derived from spectra in Figures 4, 6, and 8, shown as a function of distance. Data are also listed in Table 1. On El Centro plot, asterisk represents 180° component and diamond represents 270° component. Least-squares line through El Centro data, shown dashed, has equation $\kappa = 0.054 \text{ sec} + (0.00041 \text{ sec/km})R$, where R is the distance from epicenter. Least-squares line through Ferndale data has the equation $\kappa = 0.075 \text{ sec} + (0.00016 \text{ sec/km})R$.

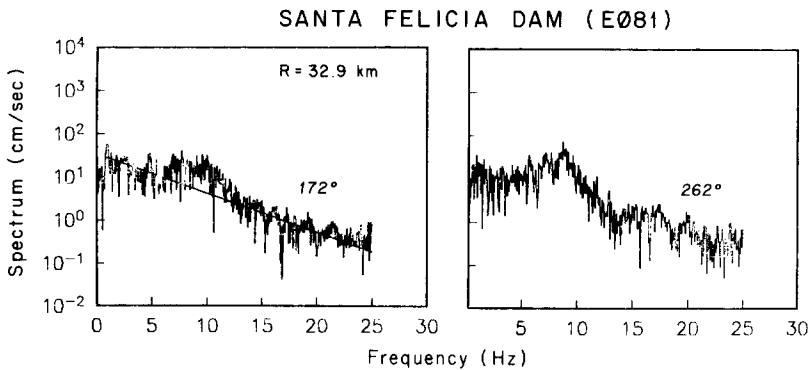


FIG. 10. *S*-wave acceleration spectra from Santa Felicia Dam for the San Fernando earthquake, showing a conspicuous site resonance superimposed on average linear trend.

These regressions suggest that exponential decay might be a general feature of the acceleration spectrum and not an artifact of the limited data set which we have studied in detail in the previous section.

A MODEL FOR THE OBSERVATIONS

Two alternative models have been proposed to explain the decay of the high frequencies in the strong motion acceleration spectrum, a phenomenon referred to by Hanks (1982) as " f_{max} ." Hanks (1982) leans toward a model in which high frequencies are generated at the seismic source, and in which attenuation, primarily caused by subsurface geological structure near the site, is responsible for the observed rapid decay of high frequencies. Papageorgiou and Aki (1983a, b) have proposed an alternative model in which the high frequency energy is not generated by the earthquake. The most straightforward explanation for the observations presented above is more in line with the Hanks (1982) model. If the S -wave displacement spectrum at the earthquake source has an ω^{-2} behavior at frequencies higher than the corner frequency (ω -square model), then attenuation within the earth is sufficient to explain the observations.

Hanks (1979) has reviewed some of the evidence for ω -square behavior and also argues that the strong motion spectra generally support this hypothesis. Modiano and Hatzfeld (1982) and Sipkin and Jordan (1980) have previously used these assumptions to study attenuation. One can define an attenuation time, t^* , for seismic phases which are modeled by rays as (Cormier, 1982)

$$t^* = \int \frac{dr}{Q_\beta(r)\beta(r)}, \quad (2)$$

and the amplitude spectrum of that phase is multiplied by the factor $e^{-\pi ft^*}$. In (2), $Q_\beta(r)$ is the spatial quality factor of shear wave attenuation, $\beta(r)$ is the shear velocity, and the integral in equation (2) is along the ray path. In general, Q_β is a function of both frequency and depth, and regional lateral variations have been observed. Converting the source spectral behavior to acceleration and incorporating the effect of attenuation leads to a spectral shape at high frequencies of

$$a(f) = A_0 e^{-\pi ft^*}. \quad (3)$$

If Q_β , and thus t^* , is independent of frequency, the effect of attenuation on an ω -square source spectrum will yield a spectral shape like equation (1).

In addition, to explain the observations, it is necessary to recognize that Q_β is a strong function of depth. The finite intercept of the trends of κ with distance (Figures 9 and 11) would then correspond to the attenuation which the S -waves all encounter in traveling through the subsurface geological structure to the surface of the earth, while the slope of the mean trend would correspond to the incremental attenuation due to predominantly horizontal propagation of S waves through the crust. Under this model, from Figures 9 and 11, attenuation caused by the subsurface geology appears to dominate the total contribution to attenuation to distances greater than 100 km.

Figure 13 illustrates several combinations of source spectral shapes and Q models. Figure 13A illustrates the ω -square spectrum behavior with four models for Q : $Q = \infty$, $Q = Q_0$, $Q = Q_1 f^1$, and $Q = Q_2 f^{0.5}$. The constants Q_1 and Q_2 are chosen so that for these two cases, $Q = Q_0$ at $f = 15$ Hz. Figure 13B illustrates the effects of the

TABLE 2
SPECTRAL DECAY PARAMETERS FOR ACCELEROGRAMS OF THE 9 FEBRUARY 1971 SAN FERNANDO, CALIFORNIA, EARTHQUAKE

Rec.	Dist. (km)	T	S	Kappa1	Peak Accel	Kappa2	Peak Accel	Rec.	Dist. (km)	T	S	Kappa1	Peak Accel	Kappa2	Peak Accel
041	9.1	10	2	0.04779	1054.9	0.04675	1148.1	157	42.5	12	0	0.06392	168.2	0.06008	116.1
048	22.4	15	0	0.08971	250.0	0.08817	131.7	166	30.8	9	1	0.05897	164.2	0.06264	147.6
051	42.8	8	0	0.05699	97.8	0.04631	122.7	171	139.8	17	1	0.08033	11.8	0.08143	16.2
054	41.9	8	0	0.06874	147.1	0.07277	117.0	176	42.9	12	0	0.05869	83.4	0.06363	115.7
056	28.6	8	1	0.07872	309.4	0.07011	265.4	179	70.7	4	1	0.03292	19.7	0.04108	49.1
057	37.1	9	0	0.09294	103.8	0.09059	148.2	180	84.3	20	0	0.08663	23.8	0.09352	29.7
058	37.1	9	0	0.06295	167.3	0.07219	207.0	183	70.8	15	1	0.05593	43.2	0.05558	56.5
059	39.8	8	0	0.07439	133.8	0.08040	147.1	184	70.8	16	1	0.06284	43.1	0.05887	57.2
062	42.8	13	0	0.06945	118.0	0.08282	130.3	185	75.6	13	1	0.08348	67.3	0.08348	67.3
065	40.0	8	1	0.09059	146.7	0.09140	155.7	186	54.1	15	0	0.08202	95.7	0.07542	96.8
068	35.0	9	0	0.07079	81.2	0.06168	98.0	187	72.1	14	0	0.06144	75.8	0.07842	56.2
071	86.0	12	0	0.03704	26.9	0.04829	25.5	188	38.9	13	0	0.06968	114.4	0.09352	126.8
072	39.5	8	1	0.05829	82.2	0.06585	115.0	191	67.8	19	1	0.10598	24.8	0.09711	40.1
075	40.1	9	0	0.08253	133.8	0.09279	111.8	192	40.7	12	1	0.04946	96.6	0.04525	98.7
078	42.5	9	1	0.05721	120.5	0.05418	189.2	195	122.6	32	0	0.08905	41.0	0.07996	30.9
081	32.9	14	1	0.06929	213.0	0.05894	198.3	196	75.4	17	0	0.09396	35.1	0.09873	31.2
083	40.0	10	0	0.07754	158.2	0.06231	161.9	197	185.7	20	0	0.08678	24.9	0.09462	34.8
086	49.4	10	0	0.07681	104.6	0.08803	80.5	198	34.0	12	2	0.05185	176.9	0.05022	167.4
087	88.5	15	0	0.08839	26.8	0.09448	28.2	199	42.0	15	0	0.05691	137.8	0.07081	238.6
088	34.1	8	1	0.07989	265.7	0.08978	209.1	204	73.8	23	0	0.08803	26.0	0.09242	20.8
089	44.0	13	0	0.06279	139.9	0.05830	139.0	205	73.6	28	0	0.09799	28.4	0.06009	28.1
092	43.1	9	1	0.05726	64.2	0.05475	79.1	206	108.2	20	0	0.08964	37.4	0.09389	44.1

095	37.4	13	0	0.06588	96.2	0.07290	83.9	207	32.8	15	2	0.06582	65.1	0.05861	97.1
098	42.7	12	0	0.05991	236.4	0.06312	192.0	208	133.4	23	1	0.08385	16.5	0.07659	17.1
101	107.6	10	0	0.09088	36.5	0.08744	29.6	210	151.4	13	0	0.06873	35.0	0.07366	39.2
102	68.5	10	2	0.05820	25.4	0.06617	21.8	214	36.2	10	1	0.07142	154.1	0.07251	156.3
103	45.4	12	0	0.04756	91.5	0.05441	120.5	217	40.0	12	0	0.08231	108.3	0.07307	88.2
104	52.2	10	1	0.07579	85.1	0.07952	103.1	220	95.8	17	1	0.09462	24.2	0.08869	34.3
105	38.7	12	0	0.07762	83.1	0.06872	77.6	221	43.3	13	2	0.04982	137.7	0.03745	165.8
106	36.1	12	2	0.05605	87.4	0.07842	188.7	222	79.3	20	0	0.09132	25.9	0.09792	25.2
107	39.8	14	0	0.05036	93.5	0.07150	107.1	223	65.0	15	2	0.08436	69.7	0.07586	53.9
108	39.8	15	0	0.08341	198.1	0.09623	181.4	231	51.7	16	0	0.06543	41.2	0.06607	37.9
110	31.5	13	1	0.05216	207.9	0.03243	138.9	233	29.3	13	0	0.06690	243.3	0.04534	197.3
112	42.5	10	0	0.04680	78.7	0.04438	101.9	236	34.9	14	0	0.06931	122.4	0.05461	167.1
114	32.3	13	0	0.06990	110.8	0.07417	136.1	239	38.4	15	0	0.06180	119.4	0.07469	161.6
115	29.3	12	0	0.07373	220.5	0.08605	146.0	241	41.8	15	1	0.05381	86.9	0.06607	137.8
118	50.2	17	0	0.08048	33.7	0.07432	32.6	244	41.9	15	1	0.07240	149.1	0.07886	126.9
121	43.1	13	0	0.05157	119.5	0.04509	112.2	246	35.7	13	0	0.05526	115.9	0.06757	107.1
124	76.2	16	0	0.09689	35.2	0.08517	34.5	248	35.7	13	0	0.06393	184.0	0.06155	174.2
128	37.1	13	0	0.05878	60.9	0.06735	91.6	249	39.2	15	0	0.05755	80.0	0.06029	84.1
131	38.2	14	0	0.07476	184.3	0.09228	160.5	251	41.8	12	1	0.07960	195.7	0.08319	188.2
134	38.9	13	0	0.06123	97.8	0.05604	82.1	253	42.0	15	0	0.06888	220.8	0.06031	242.0
137	29.0	13	0	0.04750	140.2	0.04027	128.9	255	38.9	12	1	0.08018	124.1	0.07505	128.4
141	29.6	8	2	0.07200	145.5	0.05393	108.6	258	44.6	16	0	0.06178	56.1	0.05408	83.1
142	26.8	7	2	0.03432	168.1	0.04046	143.5	261	39.6	10	0	0.05781	98.0	0.06025	107.9
143	26.6	6	2	0.02957	119.3	0.01954	109.4	262	39.0	14	1	0.09000	68.5	0.08231	93.9
144	23.3	7	1	0.06374	346.2	0.05216	277.9	265	39.9	15	1	0.06550	104.2	0.05625	125.3
145	24.9	12	0	0.08011	113.9	0.07637	103.9	266	40.0	15	0	0.05469	153.5	0.06297	129.8
148	39.9	12	1	0.06003	107.6	0.06183	112.1	267	52.0	18	0	0.05696	55.4	0.06615	61.5

same four attenuation models for a source with a displacement spectrum displaying ω^{-3} behavior (ω -cubed model). Figure 13C is for a source with ω -square behavior out to a second corner frequency f_{max} ; at higher frequencies the behavior is ω^{-6} . (Boore, 1983; Hanks, 1982). Among these combinations only the model with an ω^{-2} displacement spectrum falloff and constant Q gives the spectral trend which is modeled by equation (1). However, over finite frequency bands, the other models closely approximate exponential decay in some cases. The ω -cubed model with frequency-dependent Q is dominated by the attenuation effect at frequencies above

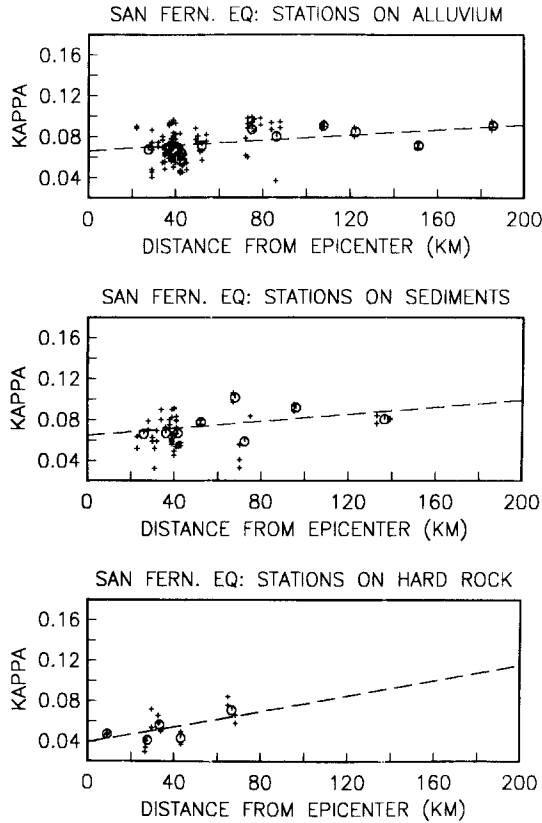


FIG. 11. Values of κ (small "+") for the frequency band 2 to 18 Hz derived from both components of San Fernando earthquake accelerograms. Data are listed in Table 2. Stations are classified as alluvium, consolidated sediments, or hard rock as in Trifunac and Brady (1975). Larger circles are at average values of both κ and distance (R) for 10-km intervals. Least-squares lines (dashed) have the following equations

alluvium	$\kappa = 0.066 \text{ sec} + (0.000126 \text{ sec/km}^{-1})R$
consolidated sediments	$\kappa = 0.065 \text{ sec} + (0.000172 \text{ sec/km}^{-1})R$
rock	$\kappa = 0.040 \text{ sec} + (0.000380 \text{ sec/km}^{-1})R$

about 5 Hz. Below 5 Hz, however, this model diverges to a level considerably above an exponential trend in contrast to data which if anything diverge below the exponential trend. The *ad hoc* model with the second corner frequency, f_{max} , is also below the exponential trend at low frequencies, but f_{max} would then be estimated to be around 5 Hz or less, rather than 10 to 15 Hz as has been suggested by Hanks (1982) and Boore (1983). Figure 13 also illustrates that if Q is proportional to f , attenuation does not affect the spectral decay parameter κ . If the dependence of Q on f is some power of f less than 1 along part of the path, then the spectral shape

may not be easily resolvable from an exponential decay. For example, if the source model is ω -square, an attenuation model with $Q \sim f^{0.25}$ (e.g., Thouvenot, 1983) would closely approximate pure exponential decay. If Q_β depends on frequency along any part of the path, then κ is not exactly t^* .

Wave propagation phenomena may also be playing a role in the determination of κ . As examples, Heaton and Helmberger (1978) have shown a theoretical example of the way plane layering and differences in the earthquake source depth can cause the spectrum to be perturbed. Correlations by Trifunac (1976) and by McGuire (1978) indicate the presence of soil amplification at low frequencies. Results by Liu (1983) suggest that the low-frequency amplification observed in alluvial valleys during the San Fernando earthquake may be a result of excitation of surface waves by the S waves incident on intervening ridges. Such phenomena are probably not sufficiently universal to explain our observations, but they probably contribute to the scatter, particularly in Figure 11. The dependence of κ on distance undoubtedly

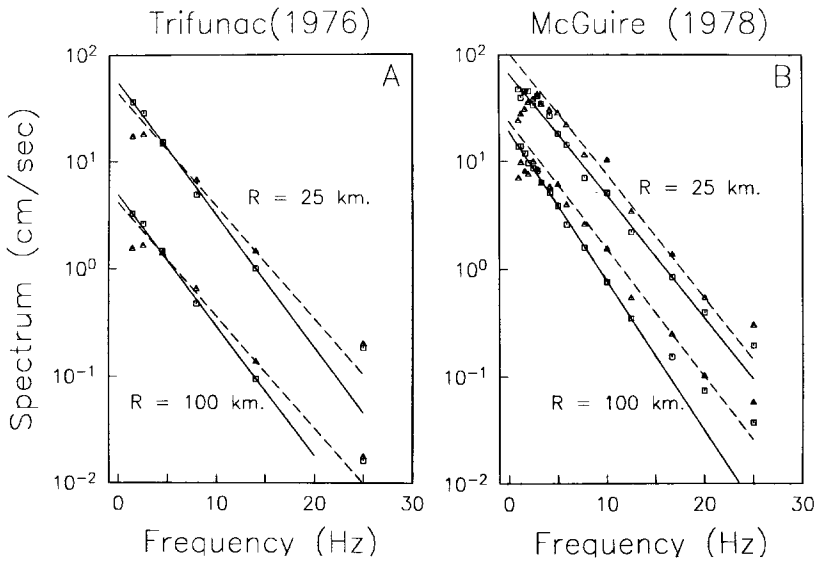


FIG. 12. (A) Discrete points are mean Fourier spectral amplitudes for a magnitude 6.5 earthquake from the regression of Trifunac (1976) at frequencies greater than 1 Hz. Lines are shown to illustrate the extent of agreement of regression points with exponential decay of the spectrum with frequency. Squares and solid lines apply to soil sites; triangles and dashed lines apply to rock sites. (B) Equivalent of (A) for the regression of McGuire (1978).

is influenced by multiple S -wave arrivals (Richter, 1958) with differing paths through the crust.

Papageorgiou and Aki (1983b) have applied several alternative models to extrapolate observations of strong motion back to the source of five earthquakes. The source models which they obtain fall off at high frequencies relative to the ω -square model. However, we do not consider that these results are sufficient to invalidate the ω -square model. If, as this paper and as Hanks (1982) have inferred, there is a highly attenuating zone near the surface, this zone will introduce a systematic effect which is not removed by the extrapolation to zero epicentral distance employed by Papageorgiou and Aki (1983a, b). For example, we observe that for the San Fernando earthquake, the source spectra derived by Papageorgiou and Aki (1983b) are consistent with exponential decay. For the attenuation model which they describe by " $Q_\beta = \text{free}$ ", all points on the source amplitude spectrum are within 25 per cent

of an exponentially decaying shape characterized by $\kappa = 0.063$ sec. Numerically, this coincides with the intercept of our linear approximations to κ as a function of distance for that earthquake for sites on alluvium (0.066 sec) and sedimentary rock (0.065 sec). This verifies that the same feature of the data which we suggest is caused by vertical propagation through shallow layers is explained by Papageorgiou and Aki as a source effect.

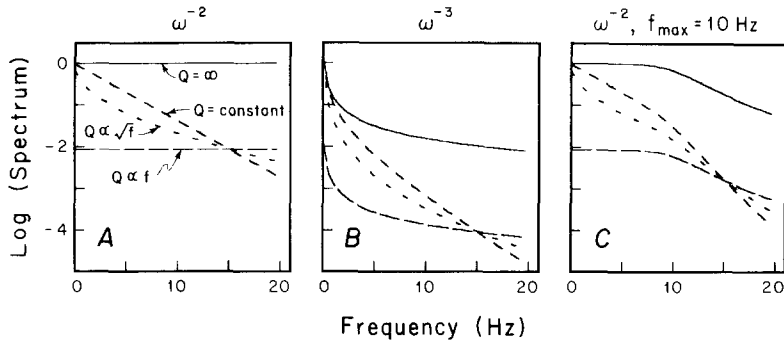


FIG. 13. Idealized acceleration spectral shapes at an accelerograph site for three source-spectral models and various attenuation models. The source spectra are described, following tradition, by falloff at high frequencies on a displacement spectrum. Thus ω^{-2} models yield a constant acceleration spectrum (A) and ω^{-3} models yield an acceleration spectrum with ω^{-1} falloff (B). Source model on right (C) consists of ω^{-2} model, but with a second corner at 10 Hz, and ω^{-4} falloff in acceleration at frequencies higher than the second corner. Attenuation models are no attenuation ($Q = \infty$), constant Q attenuation, attenuation with $Q \propto f$, and with $Q \propto f^{1/2}$.

COMPARISON WITH MODELS FOR Q IN THE CRUST

As discussed previously, it is possible to explain our observations with an ω -square source and an earth model with low, frequency-independent Q in the shallow crust. However, our model must be consistent with other recent observations that seem to show that Q depends on frequency at greater depths within the earth (e.g., Sipkin and Jordan, 1980; Aki, 1980; Singh *et al.*, 1982; Papageorgiou and Aki, 1983a, b; Dwyer *et al.*, 1983). One plausible explanation would be to appeal to models in which Q is separated into two components

$$\frac{1}{Q} = \frac{1}{Q_i} + \frac{1}{A_s f} \quad (4)$$

where the terms Q_i and $Q_s = A_s f$ represent attenuation caused by different physical mechanisms (e.g., Dainty, 1981; Rovelli, 1982). If this is true, our method would only detect the term in $1/Q_i$, and the dependence of Q_i on depth would be adjusted to fit our observations. Another possible explanation is that the frequency dependence of Q is also a function of depth (Lundquist and Cormier, 1980; Singh *et al.*, 1982). If Q is independent of frequency in the shallow crust, which dominates the attenuation of direct S waves at the distances employed in this study, then a frequency-dependent contribution to Q at depths greater than, say, 5 km would not cause a large perturbation to the exponential trend which dominates these data. In this case t^* , as a function of frequency, would be nearly equal to κ for frequencies and distances at which the shallow attenuation dominates. Of course, our analysis procedure did not allow for detection of possible frequency dependence. On these data, digitization noise could cause the same type of perturbation as frequency dependence in Q , and therefore, since our noise levels are somewhat uncertain,

interpretation of a frequency dependent perturbation to the dominant exponential trend would be unreliable.

There is some independent evidence, obtained in conjunction with seismic exploration techniques, indicating that Q is independent of frequency in the shallow crust. These studies consist of *in situ* measurements of attenuation which have employed shallow artificial sources and vertical arrays of seismometers mounted in drill holes (vertical-seismic profiles). Several studies which have concluded that Q is independent of frequency from *in situ* measurements are cited by Knopoff (1964). Additional studies which reach this conclusion include Tullos and Reid (1969), Hamilton (1972; 1976), Ganley and Kanasewich (1980), and Hauge (1981). In general, these studies have concentrated on attenuation of P waves, but McDonal *et al.* (1958) conclude that both Q_α and Q_β are independent of frequency in the Pierre Shale formation, Colorado. Frequencies considered in these studies have generally been broadband, somewhat higher (e.g., 20 to 400 Hz) than the strong-motion frequencies which we are considering. Studies which have attempted to separate the contributions from dissipation and from dispersion due to layering have concluded that dispersion is variable and sometimes important (e.g., Schoenberger and Levin, 1978), but that dissipation always makes a significant contribution (Schoenberger and Levin, 1978; Ganley and Kanasewich, 1980; Hauge, 1981; Spencer *et al.*, 1982).

Several studies, most of which employ downhole sensors have also obtained results for the attenuation as a function of depth in the shallow crust. McDonal *et al.* (1958) estimated that attenuation between the depths of 250 and 750 feet was three times as rapid as the average over the entire depth range to 4000 feet. Tullos and Reid (1969) found severe attenuation (corresponding to $Q_\alpha \sim 2$) over the depth range 1 to 10 feet in Gulf Coast sediments, but attenuation was 1 to 2 orders of magnitude less severe at depths from 10 to 100 feet. Hamilton (1976) has summarized attenuation measurements as a function of depth in sea-floor sediment. These data show a trend toward less attenuation at greater depths, but also a considerable dependence on lithology, and Hamilton suspected that lithology differences caused the overall trend of the data. Wong *et al.* (1983) find that attenuation is highly variable in the depth range 100 to 350 m of a granite pluton in Manitoba, but the overall trend is an order of magnitude decrease in attenuation rate between the top and the bottom of the hole. Thouvenot (1983) finds that Q_α increases from 40 near the surface to 600 at 7 km depth in a granite terrane in central France. Joyner *et al.* (1976) found that $Q_\beta \approx 16$ applies to the upper 186 m of sediments for a site near San Francisco Bay, and Kurita (1975) found $Q_\beta \approx 20$ for the upper crust northeast of the San Andreas fault near Hollister. Barker and Stevens (1983) found that Q_β increases rapidly with depth in the upper 50 m of sediments at three sites near El Centro in the Imperial Valley of California. A low Q surface layer for both P - and S -waves is evidently a typical, if not universal, phenomenon.

In summary, the seismic exploration results are consistent with a model that κ is closely related to t^* , and that the intercept of the trend of κ with distance is a result of relatively intense attenuation experienced by the propagation of seismic waves through subsurface geological structure below each station. This also appears to be reasonable based on the agreement of observed values of κ and calculated values of t^* based on velocity profiles and Q models. At Hollister, taking $Q = 20$ (Kurita, 1975), in conjunction with P -wave velocity models for the shallow crust northeast of the San Andreas fault in central California (e.g., Eaton *et al.*, 1970; Mayer-Rosa, 1973) and assuming Poisson's ratio is 0.25, equation (2) gives t^* between 0.088 and

0.091 sec for the upper 4 to 5 km. This range is only slightly higher than typical values of κ , about 0.085 sec, which were determined for Hollister. At El Centro, assuming κ is t^* , the intercept (Figure 9) gives $t^* = 0.054$ sec. Singh *et al.* (1982) found $t^* = 0.049$ sec for the shallow crust in the Imperial Valley and an ω -square model. These correspond to an average $Q_\beta \approx 30$ distributed over a sediment thickness of 3.8 km, using the velocity model given by curve 17 of Fuis *et al.* (1982). The slope of the least-squares line with distance, 0.00041 sec/km, corresponds to an average $Q_i \approx 800$ for shear waves below the sediments if Q is decomposed by equation (4). The slope of the least-squares line through the Ferndale data (0.00016 sec/km) suggests an average $Q_i \approx 2000$ below the high attenuation zone near the surface.

The values of κ derived for San Fernando accelerograms might suggest that the picture is not quite so simple. We observe first that if the dominant contribution to κ is from subsurface geology near the site but the increase of κ with distance is a result of propagation at depth, then one would not expect the subsurface geology to affect the slope of the relationship between κ and R . By this inference, the possibly different slopes which are derived for different types of site conditions would have to result from sample differences. It was pointed out previously that this may be the case. We notice that the slope is greatest for rock sites which are only represented at relatively short distances, while the slope is smallest for alluvium sites which are represented to the greatest distances. These observations suggest the possibility that the slope, $d\kappa/dR$, is a decreasing function of distance. There is no theoretical reason for $d\kappa/dR$ to be independent of distance, and our linear regressions were intended only to illustrate general trends. It may be possible to invert κ and $d\kappa/dR$ as a function of distance to derive Q_i as a function of depth. The average slopes shown in Figure 11 correspond to Q_i greater than 1000 at depth.

A visual survey of the spectra which we have employed does allow the possibility that a frequency dependence in Q at depth contributes to the spectral shape at low frequencies ($f < f_E \approx 5$ Hz). Such frequency dependence might cause some spectra to appear flat or to increase with frequency at these lowest frequencies. We have indicated previously that a deviation from exponential decay might be present in Figures 1 and 2 at $f < 5$ Hz. This frequency band might instead be characterized by the source spectrum not yet approaching its asymptotic ω -square form due to a complex source mechanism which introduces a second corner frequency (e.g., Joyner, 1984). A thorough study focused on these frequencies seems appropriate. A model in which Q is strictly proportional to frequency at all depths would seem to be ruled out, however, since such a model is not consistent with the observed increase of κ with distance.

RELATIONSHIP TO f_{\max}

We have designated the observational range of validity of equation (1) as $f > f_E$, where f_E is a label for the low frequency limit of agreement. On some spectra f_E is closely related to f_0 while in others it seems to be a conspicuous feature occurring at a distinctly larger frequency than f_0 . Where f_0 and f_E differ significantly, the processes which dominate the spectrum between f_0 and f_E remain to be determined.

The frequency f_E is distinguishably smaller than f_{\max} . f_{\max} is recognized on log-log axes as a frequency above which spectral amplitudes appear to diminish abruptly. For California accelerograms from moderate- to large-sized earthquakes, f_E is generally less than 5 Hz (examples are in Figures 1, 2, 4, 6, and 8) while f_{\max} generally occurs in the frequency band 10 to 20 Hz (Hanks, 1982). f_{\max} , in the sense used by Hanks, has been employed as an integration limit to derive root-mean-

square acceleration from a parametric model for the acceleration spectrum (Hanks, 1979; McGuire and Hanks, 1980; Hanks and McGuire, 1981; Boore, 1983). To preserve this function f_{\max} needs to be at a frequency where the spectral trend has fallen to a value of the order of 0.1 to 0.3 of its peak. This implies that $f_{\max} \approx \text{constant}/\kappa$ or perhaps $f_{\max} \approx f_E + \text{constant}/\kappa$ where the constant is on the order of 0.2 to 0.7 depending on the shape of the spectrum. If f_{\max} is chosen in this manner, the mathematical properties of the exponential curve make the spectrum observationally indistinguishable from a constant for frequencies greater than f_E but less than some fraction, on the order of 0.2 to 0.5, of f_{\max} .

As recognized on the source spectra which have been derived by Papageorgiou and Aki (1983a, b), f_{\max} is generally smaller, with numerical values between 2.5 and 5 Hz. Thus, this usage of f_{\max} is consistent with the frequency range found for f_E on some spectra. However, our interpretations are opposite. While Papageorgiou and Aki (1983a, b) suggest that the source acceleration spectrum is a constant for $f < f_{\max}$ and falls off above f_{\max} , our interpretation is that the source spectrum is a constant for $f > f_E$, but may not be constant for f between f_0 and f_E .

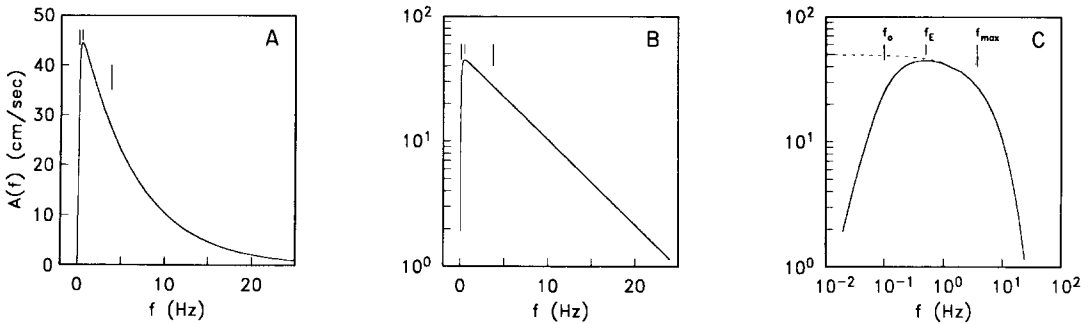


FIG. 14. A particular spectral shape plotted on three types of axes. Fiducials identify f_0 , f_E , and f_{\max} in each frame.

Figure 14 shows a Brune (1970) spectrum modified by exponential decay at all frequencies

$$a(f) = (\text{constant}) \frac{f^2}{1 + \left(\frac{f}{f_0}\right)^2} e^{-\pi\kappa f}. \tag{5}$$

In Figure 14, the parameters which have been employed are $f_0 = 0.1$ Hz and $\kappa = 0.05$ sec. Figure 14A uses algebraic axes, 14B uses semi-logarithmic axes, and 14C uses logarithmic axes. An exponential function, starting at $f = 0$ and with the same high-frequency asymptote, is shown as a dashed line in Figure 14C. In 14B, the frequency f_E is recognized by a deviation from the straight line defined at higher frequencies. In 14C, f_{\max} is picked according to the convention described above: the integral from 0 to f_{\max} of a constant spectrum with amplitude equal to the peak of this spectrum gives the same value of a_{rms} as the spectrum plotted in Figure 14. Qualitative picks of f_{\max} as the corner of the exponential curve may differ from the value shown. At the value of f_E shown, the spectrum described by equation (5) differs from the exponential curve by about 4 per cent.

For spectra described by (5), f_E is related to f_0 . For more complex spectra, such as the two-corner source spectra proposed by Joyner (1984), a direct relationship no longer exists.

CONCLUSIONS

At high frequencies, the Fourier acceleration spectrum of S waves decays exponentially in a majority of existing California accelerograms. The spectral decay parameter, κ , was defined in equation (1), and a study of its properties was pursued in this paper. The principal features of the spectral decay parameter are: (1) it can be used to describe the shape of the Fourier amplitude spectrum of acceleration in the frequency band from ~ 2 Hz to at least 20 Hz; (2) it seems to be primarily an effect caused by subsurface geological structure near the site because it is only a weak function of distance; and (3) it seems to be smaller on rock sites than on sites of less competent geology. These observations suggest that the spectral decay parameter is related to attenuation within the earth, and that all of the earthquake sources employed for our study produce the same asymptotic behavior of the spectral shape at high frequencies.

We have attributed deviations from a trend of exponential decay at high frequencies to two sources, broadband site resonances and noise. The obvious site resonances, such as in Figure 10, appear on about 10 per cent of the San Fernando accelerograms. Weaker resonances may add some noise to determinations of κ . Figure 2 shows a clear example of the effect of digitization noise on the spectrum, and we have inferred that spectra in Figures 4, 6, and 8 approach a level trend because of digitization or instrumental noise. At low frequencies, it is possible that frequency dependence in Q is also causing a deviation from the exponential decay on some records.

Our model for the origin of the spectral decay parameter envisions a frequency-independent contribution to the attenuation parameter Q which modifies the shape of source displacement spectrum obeying an ω^{-2} asymptotic behavior at high frequencies. The dominant contribution to κ would be attenuation close to the accelerograph site; this contribution is less severe for more competent site geologies. There is also a small incremental attenuation which results from lateral propagation in the crust. This attenuation mechanism implies that the source spectrum is modified by $e^{-\pi\kappa f}$ at low frequencies ($f < f_E$) also, but that other processes dominate the shape. Based on the data presented in this paper, we cannot rule out a hybrid model in which the spectrum falls off due to both source and attenuation effects, but significantly smaller values of κ will be forthcoming from sites on more competent rock than those studied here. Thus, future studies of this type will eventually place constraints on the extent to which the source spectrum deviates from the ω -square model.

Several research topics remain to be addressed. These include the relationship of κ to site geology including research into nonlinear effects, studies to reduce scatter about attenuation equations, and elaboration of the relationship between κ and attenuation including possible inversion of κ -distance observations for attenuation as a function of depth.

ACKNOWLEDGMENTS

K. Aki, J. E. Luco, O. W. Nuttli, and M. Reichle provided helpful critical reviews of this manuscript. We thank T. C. Hanks for calling our attention to the article by Berrill and Hanks, as well as for a thoughtful review of the manuscript. We also wish to acknowledge helpful discussions with J. N. Brune, T. H. Heaton, A. H. Olson, and D. M. Boore. P. Bodin provided much assistance in gathering information for this study. This research was supported by National Science Foundation Grant CEE 81-20096.

REFERENCES

- Aki, K. (1980). Attenuation of shear-waves in the lithosphere for frequencies from 0.05 to 25 Hz, *Phys. Earth Planet. Interiors* **21**, 50–60.
- Anderson, J. G. (1984). The 4 September 1981 Santa Barbara Island, California, earthquake: interpretation of strong motion data, *Bull. Seism. Soc. Am.* **74**, 995–1010.
- Anderson, J. G., J. Prince, J. N. Brune, and R. S. Simons (1982). Strong motion accelerograms, in J. G. Anderson and R. S. Simons, Editors, The Mexicali Valley Earthquake of 9 June 1980, *Newsletter Earthquake Eng. Res. Inst.* **16**, 79–83.
- Barker, T. G. and J. L. Stevens (1983). Shallow shear wave velocity and Q structures at the El Centro strong motion accelerograph array, *Geophys. Res. Letters* **10**, 853–856.
- Berrill, J. B. (1975). A study of high-frequency strong ground motion from the San Fernando earthquake, *Ph.D. Thesis*, California Institute of Technology, Pasadena, California.
- Berrill, J. B. and T. C. Hanks (1974). High frequency amplitude errors in digitized strong motion accelerograms, in *Analysis of Strong Motion Earthquake Accelerograms*, volume IV—Fourier Amplitude Spectra, Parts Q, R, S—Accelerograms IIQ 233 through IIS 273, Report EERL 74-104, Earthquake Engineering Research Laboratory, California Institute of Technology, Pasadena, California.
- Bodle, R. R. (1944). *United States Earthquakes 1942*, Serial 662, U.S. Dept. of Commerce, Coast and Geodetic Survey, Washington, D.C.
- Boore, D. M. (1983). Stochastic simulation of high frequency ground motions based on seismological models of the radiated spectra, *Bull. Seism. Soc. Am.* **73**, 1865–1894.
- Brune, J. N. (1970). Tectonic stress and the spectra of seismic shear waves from earthquakes, *J. Geophys. Res.* **75**, 4997–5009.
- Cormier, V. F. (1982). The effect of attenuation on seismic body waves, *Bull. Seism. Soc. Am.* **72**, S169–S200.
- Dainty, A. M. (1981). A scattering model to explain seismic Q observations in the lithosphere between 1 and 30 Hz, *Geophys. Res. Letters* **8**, 1126–1128.
- Dobrin, M. B. (1960). *Introduction to Geophysical Prospecting*, 2nd ed., McGraw-Hill, New York, 446 pp.
- Dwyer, J. J., R. B. Hermann, and O. W. Nuttli (1983). Spatial attenuation of the L_g wave in the central United States, *Bull. Seism. Soc. Am.* **73**, 781–796.
- Earthquake Engineering Research Laboratory (1971). Strong Motion Earthquake Accelerograms Volume II—Corrected accelerograms and integrated ground velocity and displacement curves, Report EERL 71-50, California Institute of Technology, Pasadena, California.
- Eaton, J. P., M. E. O'Neill, and J. N. Murdock (1970). Aftershocks of the 1966 Parkfield-Cholame, California, earthquake: a detailed study, *Bull. Seism. Soc. Am.* **60**, 1151–1197.
- Fuis, G. S., W. D. Mooney, J. H. Healey, G. A. McMechan, and W. J. Lutter (1982). Crustal structure of the Imperial Valley region, in *The Imperial Valley, California, earthquake of October 15, 1979*, *U.S. Geol. Surv. Profess. Paper 1254*, 25–50.
- Ganley, D. C. and E. R. Kanasewich (1980). Measurement of absorption and dispersion from check shot surveys, *J. Geophys. Res.* **85**, 5219–5226.
- Hamilton, E. L. (1972). Compressional-wave attenuation in marine sediments, *Geophysics* **37**, 620–646.
- Hamilton, E. L. (1976). Sound attenuation as a function of depth in the sea floor, *J. Acoust. Soc. Am.* **59**, 528–535.
- Hanks, T. C. (1975). Strong ground motion of the San Fernando, California, earthquake: ground displacements, *Bull. Seism. Soc. Am.* **65**, 193–226.
- Hanks, T. C. (1979). b -values and $\omega^{-\gamma}$ seismic source models: implications for tectonic stress variations along active crustal fault zones and the estimation of high-frequency strong motion, *J. Geophys. Res.* **84**, 2235–2242.
- Hanks, T. C. (1982). f_{\max} , *Bull. Seism. Soc. Am.* **72**, 1867–1880.
- Hanks, T. C. and R. K. McGuire (1981). The character of high-frequency strong ground motion, *Bull. Seism. Soc. Am.* **71**, 2071–2096.
- Hauge, P. S. (1981). Measurements of attenuation from vertical seismic profiles, *Geophysics* **46**, 1548–1558.
- Heaton, T. H. and D. V. Helmberger (1978). Predictability of strong ground motion in the Imperial Valley: modeling the M 4.9, November 4, 1976 Brawley earthquake, *Bull. Seism. Soc. Am.* **68**, 31–48.
- Hileman, J. A., C. R. Allen, and J. M. Nordquist (1973). *Seismicity of the southern California region*. 1 January 1932 to 31 December 1972, Seismological Laboratory, California Institute of Technology,

- Pasadena, California.
- Jennings, C. W. (1975). *Fault Map of California*, Map No 1, Faults, Volcanos, Thermal Springs and Wells, California Division of Mines and Geology, Sacramento, California.
- Joyner, W. B. (1984). A scaling law for the spectra of large earthquakes, *Bull. Seism. Soc. Am.* **74**, 1167–1188.
- Joyner, W. B., R. E. Warrick, and A. A. Oliver, III (1976). Analysis of seismograms from a downhole array in sediments near San Francisco Bay, *Bull. Seism. Soc. Am.* **66**, 937–958.
- Knopoff, L. (1964). *Q*, *Rev. Geophys.* **2**, 625–660.
- Kurita, T. (1975). Attenuation of shear waves along the San Andreas fault zone in central California, *Bull. Seism. Soc. Am.* **65**, 277–292.
- Leeds, A. (1979). The locations of the 1954 northern Baja California earthquake, *Masters Thesis*, University of California at San Diego, La Jolla, California.
- Liu, H.-S. (1983). Interpretation of near-source ground motion and implications, *Ph.D. Thesis*, California Institute of Technology, Pasadena, California, 184 pp.
- Lundquist, G. M. and V. C. Cormier (1980). Constraints on the absorption band model of *Q*, *J. Geophys. Res.* **85**, 5244–5256.
- Mayer-Rosa, D. (1973). Travel-time anomalies and distribution of earthquakes along the Calaveras fault zone, California, *Bull. Seism. Soc. Am.* **63**, 713–729.
- McDonal, F. J., F. A. Angona, R. L. Mills, R. L. Sengbush, R. G. Van Nostrand, and J. E. White (1958). Attenuation of shear and compressional waves in Pierre Shale, *Geophysics* **23**, 421–439.
- McGuire, R. K. (1978). A simple model for estimating Fourier amplitude spectra of horizontal ground acceleration, *Bull. Seism. Soc. Am.* **69**, 803–822.
- McGuire, R. K. and T. C. Hanks (1980). RMS accelerations and spectra amplitudes of strong ground motion during the San Fernando, California, earthquake, *Bull. Seism. Soc. Am.* **70**, 1907–1919.
- Modiano, T. and D. Hatzfeld (1982). Experimental study of the spectra content for shallow earthquakes, *Bull. Seism. Soc. Am.* **72**, 1739–1758.
- Murphy, L. M. and F. P. Ulrich (1951a). *United States Earthquakes 1948*, U.S. Dept. of Commerce, Serial 746, Coast and Geodetic Survey, Washington, D.C.
- Murphy, L. M. and F. P. Ulrich (1951b). *United States Earthquakes 1949*, Serial 748, U.S. Dept. of Commerce, Coast and Geodetic Survey, Washington, D.C.
- Murphy, L. M. and W. K. Cloud (1954). *United States Earthquakes 1952*, Serial 773, U.S. Dept. of Commerce, Coast and Geodetic Survey, Washington, D.C.
- Murphy, L. M. and W. K. Cloud (1955). *United States Earthquakes 1953*, U.S. Dept. of Commerce, Coast and Geodetic Survey, Washington, D.C.
- Papageorgiou, A. S. and K. Aki (1983a). A specific barrier model for the quantitative description of inhomogeneous faulting and the prediction of strong ground motion. Part I. Description of the model, *Bull. Seism. Soc. Am.* **73**, 693–722.
- Papageorgiou, A. S. and K. Aki (1983b). A specific barrier model for the quantitative description of inhomogeneous faulting and the prediction of strong ground motion. Part II. Applications of the model, *Bull. Seism. Soc. Am.* **73**, 953–978.
- Real, C. R., T. R. Toppozada, and D. L. Parke (1978). *Earthquake Epicenter Map of California*, Map Sheet 39, California Division of Mines and Geology, Sacramento, California.
- Richter, C. F. (1958). *Elementary Seismology*, W. H. Freeman and Co., San Francisco, California.
- Rovelli, A. (1982). On the frequency dependence of *Q* in Friuli from short-period digital records, *Bull. Seism. Soc. Am.* **72**, 2369–2372.
- Sacks, I. S. (1980). Mantle *Q* from body waves—Difficulties in determining frequency dependence, (abstract), *EOS, Trans. Am. Geophys. Union* **61**, 299.
- Schoenberger, M. and F. K. Levin (1978). Apparent attenuation due to intrabed multiples. II. *Geophysics* **43**, 730–737.
- Singh, S. K., R. J. Apsel, J. Fried, and J. N. Brune (1982). Spectral attenuation of *SH* waves along the Imperial fault, *Bull. Seism. Soc. Am.* **72**, 2003–2016.
- Sipkin, S. A. and T. H. Jordan (1980). Regional variation of Q_{SES} , *Bull. Seism. Soc. Am.* **70**, 1071–1102.
- Spencer, T. W., J. R. Sonnad, and T. M. Butler (1982). Seismic *Q* Stratigraphy or dissipation, *Geophysics* **47**, 16–24.
- Thouvenot, F. (1983). Frequency dependence of the quality factor in the upper crust: a deep seismic sounding approach, *Geophys. J. R. Astr. Soc.* **73**, 427–447.
- Trifunac, M. D. (1976). Preliminary empirical model for scaling Fourier amplitude spectra of strong ground accelerations in terms of earthquake magnitude, source to station distance, and recording site conditions, *Bull. Seism. Soc. Am.* **66**, 1343–1373.

- Trifunac, M. D. and V. W. Lee (1978). Uniformly processed strong earthquake ground accelerations in the western United States of America for the period from 1933 to 1971: corrected acceleration, velocity and displacement curves, Report CE 78-01, Department of Civil Engineering, University of Southern California, Los Angeles, California.
- Trifunac, M. D. and A. C. Brady (1975). On the correlation of seismic intensity scales with peaks of recorded strong ground motion, *Bull. Seism. Soc. Am.* **65**, 139-162.
- Tullos, F. N. and A. C. Reid (1969). Seismic attenuation of Gulf Coast sediments, *Geophysics* **34**, 516-528.
- Wong, J., P. Hurley, and G. F. West (1983). Crosshole seismology and seismic imaging in crystalline rocks, *Geophys. Res. Letters* **10**, 686-689.

INSTITUTE OF GEOPHYSICS AND PLANETARY PHYSICS (A-025)
SCRIPPS INSTITUTION OF OCEANOGRAPHY
UNIVERSITY OF CALIFORNIA, SAN DIEGO
LA JOLLA, CALIFORNIA 92093

Manuscript received 11 October 1983